

# Blocking Performance of Multi-rate OCDMA PONs with QoS Guarantee

John S. Vardakas\*, Ioannis D. Moscholios<sup>†</sup>, Michael D. Logothetis\*, and Vassilios G. Stylianakis\*

\*WCL, Dept. of Electrical and Computer Engineering

University of Patras, Patras, 265 04, Greece,

Emails: {jvardakas, m-logo, stylian}@wcl.ee.upatras.gr

<sup>†</sup>Dept. of Telecommunications Science and Technology

University of Peloponnese, 221 00, Tripolis, Greece,

Email: idm@uop.gr

**Abstract**—In this paper, we propose a new teletraffic model for the calculation of blocking probabilities in an Optical Code Division Multiple Access (OCDMA) Passive Optical Network (PON) supporting multiple service-classes of Poisson traffic. OCDMA is a promising candidate of PON configuration for the provision of moderate security communications with large dedicated bandwidth to each end user. The PON accommodates multiple service-classes that are differentiated by either different data-rates or different Quality of Service levels. Parameters related to the additive noise, multiple access interference and user activity are incorporated into our analysis. Based on a two-dimensional Markov chain, we propose a recursive formula for the calculation of the number of in-service codewords, when the OCDMA PON guarantees Quality of Service (QoS), or not. To evaluate the proposed model, the analytical results are compared with simulation results to reveal that the model's accuracy is quite satisfactory.

**Keywords**—Passive Optical Network; Optical Code Division Multiple Access; Multiple Access Interference; Blocking Probability; Quality of Service; Parallel Mapping.

## I. INTRODUCTION

The exponential growth of the Internet traffic volume and popularity of broadband applications have accelerated the demand for higher data rates. In backbone networks the capacities have been significantly increased, mainly due to the utilization of the Wavelength Division Multiplexing (WDM) with hundreds of channels in each optical fiber. On the other hand, current solutions in the access domain, such as the Digital Subscriber Line (DSL), are inadequate to deal with the growing bandwidth-hungry applications. To break the bottleneck between the access networks and the ultrahigh-speed backbone networks, high capacity and cost effective access solutions are required. The Passive Optical Network (PON) has received a tremendous attention from both academic [1] and industrial [2] communities, mainly due to the low operational cost, the enormous bandwidth offering and the absence of active components between the central office and the customer's premises.

Over the years, several standards for PONs have been evolved, in the form of the G.983 ITU-T recommendations, which include Asynchronous Transfer Mode PONs (ATM-PONs) and Broadband PONs (BPONs) [3], or in the form of

IEEE 802.3ah for the Ethernet PON (EPON) [4], etc. These PONs are based on a Time Division Multiple Access (TDMA) scheme and they typically use a 1550 nm wavelength for downstream and a 1310 nm for upstream [5]. While these TDMA-PONs employ two wavelengths for the upstream and downstream direction, respectively, the WDM-PON utilizes multiple wavelengths, so that two wavelengths are allocated to each user for down/upstream transmissions. A different approach for the provision of multiple access in PONs is the Optical Code Division Multiple Access (OCDMA). In contrast to the other multiple access schemes, OCDMA can multiplex a number of channels on the same wavelength and on the same time-slot [6]. In addition, OCDMA offers full asynchronous transmission, soft capacity on demand, low latency access, simple network control and better security against unauthorized access [7].

In OCDMA, each communication channel is distinguished by a specific optical code. At the receiver each data is multiplied by a unique code sequence either in the time domain [8], or in the wavelength domain [9], or in a combination of both (simultaneously) [10]. The decoder receives the sum of all encoded signals from different transmitters and recovers the data from a specific encoder, by using the same optical code. All the remaining signals appear as noise to the specific receiver; this noise is known as multiple access interference (MAI) and is the key degrading factor of the network's performance. Apart from MAI, other forms of additive noise deteriorate the network performance, such as beat noise, shot noise, thermal noise and fiber-link noise, and worth considering them in performance analysis [11].

Service differentiation in OCDMA networks can be performed by considering either different data-rates or different QoS levels for the supported service-classes. For the provision of data-rate differentiation several solutions have been investigated. A simple approach is based on the utilization of multi-length codes [12]; however, under multi-length coding, short-length codes introduce significant interference over long-length codes, while high error probability emerges for high rate users. Optical fast-frequency hopping has been also proposed for multi-rate OCDMA networks [13]. This technique is based on multiple wavelengths, which requires multi-wavelength

transmitters with high sensitivity on power control. Another way to provide data-rate differentiation is the assignment of several codes to each service-class. This procedure is known as the parallel mapping technique [14]. In this case the number of codes is proportional to the data rate of the assigned service-class. For the provision of differential QoS, one-dimensional and two-dimensional variable-weight optical codes have been introduced in order to control the Bit Error Rate (BER) at the receiver [15], [16].

A call-level performance analysis of an OCDMA PON supporting multiple service-classes of infinite traffic source population, appears in [17]. The shared medium (link between Optical Line Terminal (OLT) and Passive Optical Splitter/Combiner (PO-SC), see Fig. 1) is modelled by a two dimensional Markov chain. Based on this chain, an approximate recursive formula for the calculation of blocking probabilities in the PON is presented. However, in [17], no mathematical proof is provided for the recursive formula; its proof appears in [1]. To prove it, we rely on the distribution of the occupied bandwidth in the PON, which is calculated recursively. The analysis takes into account the user activity, by incorporating different service times for active and passive (silent) periods. The capacity of the PON is defined by the total number of codewords assigned to active users. An arriving call is blocked, if the resulting number of codewords assigned to all in-service calls exceeds a predefined threshold which represents the PON capacity. This case defines the Hard Blocking Probability (HBP). A call may also be blocked in any other system state due to the existence of different forms of additive noise (thermal noise, shot noise, beat noise). The latter case is expressed by the Local Blocking Probability (LBP).

In this paper, (a) we include the analysis presented in [1] and [17], (b) we provide further evaluation of the proposed loss model, and (c) we extend our analysis (and the evaluation) to cover the case of a multi-rate OCDMA PON that provides QoS support. The QoS differentiation is performed by considering variable-weight code lengths, in order to achieve different BER levels at the receiver. Furthermore, we calculate the link utilization in the PON either without, or with QoS support. Finally, in both cases, we provide the analysis for the determination of the Burst Blocking Probability (BBP), which is the probability that a call cannot return to the active state from the passive state, due to the unavailability of codewords, or due to the presence of additive noise. The accuracy of the proposed methodology is evaluated through simulation and is found to be quite satisfactory.

The rest of the paper is organized as follows. In Section II, we discuss about related works. In Section III, we present the system model. In Section IV, we present the recursive formula for the calculation of blocking probabilities in a multi-rate OCDMA PON. This analysis is extended in Section V, in order to cover the case of multiple service-classes with different QoS levels. Section VI is the evaluation section. We conclude in Section VII.

## II. RELATED WORKS

There is a significant research activity on OCDMA networks, but it is mainly focused on the performance of several OCDMA components, and not on the teletraffic performance of the overall network, like a PON. Only a few analytical models have been presented in the literature involving the computation of blocking probabilities in OCDMA networks.

Goldberg and Prucnal [18] provide analytical models for the determination of blocking probabilities and for the teletraffic capacity in OCDMA networks. The results of paper [18] are applicable to OCDMA PONs, too. The capacity of the OCDMA PON can be defined by the traditional way, as the number of continuously transmitting users, which depend on the number of codewords that the PON supports, given that each user needs a codeword. Obviously, when the number of users exceeds the number of codewords in the PON, call blocking occurs. The PON capacity is limited not only due to the limited number of codewords, but also due to the presence of MAI, as well as due to additive noise in OCDMA PONs. In [18], only the MAI is taken into account. Due to MAI, when the number of transmitting users in the PON becomes excessive, the BER at the receiver degrades, causing an outage; that is, blocking occurs. The number of users is assumed constant (instead of considering Poisson arrivals). In addition, the authors take into account in the analysis the stochastic nature of the offered traffic by a user. As it is clearly stated in [18], the proposed analysis is independent of the spreading code used by the OCDMA network. However, it has the important limitation of considering just one service-class.

A similar study is performed in [19]. It is concentrated on the performance analysis of the teletraffic capacity of a hybrid WDM/DS(Direct Sequence)-PON. In such a PON, for each wavelength, each user data bit is temporarily encoded with a given sequence of pulses. By this temporal encoding, the same codewords are shared among different users; thus many users can simultaneously communicate with each other by using the same restricted number of codewords. In other words, the user capacity performance is increased in a cost effective way per wavelength for a hybrid WSM/DS-OCDMA PON configuration. In determining the teletraffic capacity of this PON, two considerations are taken into account: (a) The so called nominal resource capacity, which is defined as the maximum number of resources both in WDM and OCDMA system, that is: (number of wavelengths) x (number of codewords). (b) The so called simultaneous user capacity in OCDMA system, defined as the maximum simultaneous transmitting users at acceptable BER performance. As in [18], it is also assumed in [19] that only the MAI affects the BER. Blocking occurs when the system reaches either its nominal resource capacity or the simultaneous user capacity. It is shown that the blocking (and teletraffic capacity) performance depends on the code family used in the OCDMA system. Again, this paper considers a single service-class, which is a serious limitation in the study of broadband networks, like PONs.

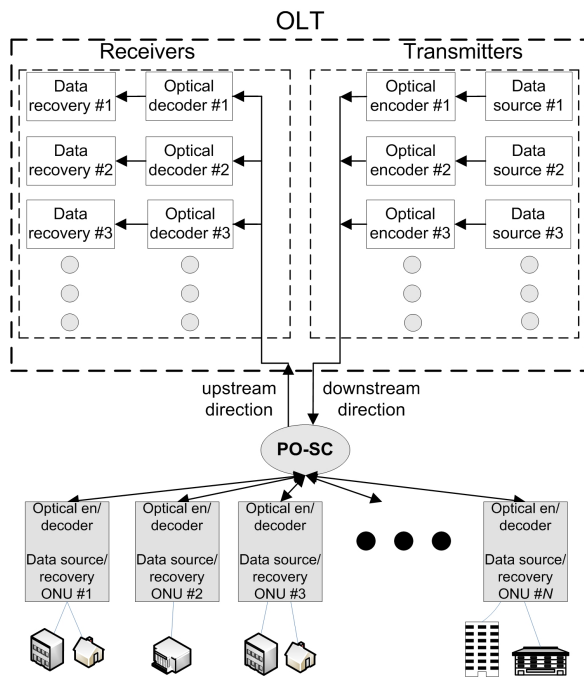


Fig. 1. A basic configuration of an OCDMA PON.

We also provide a call-level analysis of hybrid WDM-OCDMA PONs [20], to determine connection failure probabilities due to unavailability of a wavelength in the considered WDM system with dynamic wavelength assignments, and call blocking probabilities due to the MAI of the OCDMA system. The springboard of the analysis presented in [20] is well-established teletraffic models, developed for Wireless CDMA systems [21].

### III. SYSTEM MODEL OF A MULTI-RATE OCDMA PON

We consider the OCDMA PON of Fig. 1. A number of Optical Network Units (ONUs) located at the users' premises are connected to an OLT (located to Central Office) through a PO-SC (quite close to the ONUs). The PO-SC is responsible for the broadcasting of traffic from the OLT to the ONUs (downstream direction) and for the grouping of data from the ONUs and the transmission of the collected data to the OLT through one fiber (upstream direction). We study the upstream direction; however, the following analysis can be applied to the downstream direction. Users which are connected to an ONU, switch between active and passive (silent) periods. The PON utilizes  $(L, W, \lambda_a, \lambda_c)$  codewords, which have the same length  $L$ , the same  $W$ , while the auto-correlation  $\lambda_a$  and the cross-correlation  $\lambda_c$  parameters are defined according to the desired value of the BER at the receiver. The PON supports  $K$  service-classes. The service-differentiation in this OCDMA system is realized using the parallel mapping technique. Under this technique, the OLT assigns  $b_k$  codewords to a service-class  $k$  call that is accepted for service and these codewords are used by the call for its entire duration. In particular, during a service-class  $k$  call,  $b_k$  data bits are transmitted in parallel in

each bit period. One codeword is used in order to encode data bit "1", while data bit "0" is not encoded. Therefore, in each bit period at most  $b_k$  data bits are encoded and this number is equal to the number of "1" data bits that are transmitted during this bit period. In this way, we avoid the complex procedure of assigning codewords to calls in each bit period. Also, the data rate of service-class  $k$  is equal to  $b_k \cdot D$ , where  $D$  is the data rate of a single codeword call, since  $b_k$  data bits are transmitted in parallel during a bit period.

When a single codeword is applied to an active call, the received power of this call at the receiver is denoted by  $I_{unit}$ , where  $I_{unit}$  corresponds to the received power per bit, for a specific value of BER. Since different service-classes require different data-rates, the maximum interference  $I_k$  that an active service-class  $k$  call causes to the receiver is proportional to  $I_{unit}$ , because  $b_k$  data bits of service-class  $k$  are transmitted in parallel, during a bit period, therefore:

$$I_k = b_k \cdot I_{unit} \quad (1)$$

This maximum value of the received power of a service-class  $k$  call refers to the power of the call when all  $b_k$  parallel bits are "1".

Calls that are accepted for service, start an active period and may constantly remain in the active state for the entire duration of the call, or alternate between active and passive states. Throughout an active state, the traffic source sends bursts, while during a passive state no transmission of data occurs. When a call is transferred from the active state to the passive state, the number of codewords that this call was utilizing in its active state are released, and these codewords become available to new arriving calls. When a call attempts to become active again, it re-requests the same number of codewords (as in the previous active state); if the total number of codewords of all in-service calls does not exceed a maximum value, a new active period begins; if not, burst blocking occurs and the call remains in the passive state. At the end of the active period the total number of codewords held by all in-service calls is reduced by  $b_k$  and the call either jumps to the passive state with probability  $v_k$ , or departs from the system with probability  $1 - v_k$ . Furthermore, calls that belong to service-class  $k$  arrive to an ONU according to a Poisson process; the total arrival rate from all ONUs is denoted  $\lambda_k$ . The service time of service-class  $k$  calls in state  $i$ , ( $i=1$  indicates the active state,  $i=2$  the passive state) is exponentially distributed with mean  $\mu_{ik}^{-1}$ .

#### A. Local Blocking Probabilities

According to the principle of the CDMA technology, a call should be blocked if it increases the noise of all in-service calls above a predefined level, given that a call is noise for all other calls. This noise is known as MAI. We distinguish the MAI from other forms of noise, the shot noise, the beat noise, the thermal noise and the fiber-link noise. The thermal noise is generally modelled as Gauss distribution  $(0, \sigma_{th})$ , the fiber-link noise is modelled as Gauss distribution  $(0, \sigma_{fb})$  [22], while the beat noise is also modelled as a Gauss distribution

$(0, \sigma_b)$  [11]. The shot noise is modelled as a Poisson process where its expectation and variance are both denoted by  $p$  [22]. According to the central limit theorem, we can assume that the additive shot noise is modelled as Gauss distribution  $(\mu_N, \sigma_N)$ , considering that the number of users in the PON is relatively large. Therefore, the interference  $I_N$  caused by the four types of noise is modelled as a Gaussian distribution with mean  $\mu_N = p$  and variance  $\sigma_N = \sqrt{\sigma_{th}^2 + \sigma_{fb}^2 + \sigma_b^2 + p^2}$ .

The Call Admission Control (CAC) in the OCDMA PON under consideration is performed by measuring the total received power at the receiver. When a new call arrives (which automatically enters an active state), the CAC checks the total received power and if it exceeds a maximum value  $I_{\max}$ , the call is blocked and lost. This condition is expressed by the following relation:

$$\sum_{k=1}^K (n_k^1 I_k \cdot P_{\text{interf}}) + I_k + I_N > I_{\max} \Leftrightarrow \quad (2)$$

$$\frac{I_N}{I_{\max}} > 1 - \sum_{k=1}^K (n_k^1 \frac{I_k}{I_{\max}} \cdot P_{\text{interf}}) - \frac{I_k}{I_{\max}}$$

where  $n_k^1$  represent the number of the service-class  $k$  calls in the active system and  $P_{\text{interf}}$  is the probability of interference. This probability is a function of the maximum cross-correlation parameter  $\lambda_c$ , the weight  $W$  and the length  $L$  of the codewords and the hit probabilities between two codewords that are used to encode data bits of different users. The hit probabilities  $p_{\lambda_c, i}$  of getting  $i$  hits during a bit period out of the maximum cross-correlation value  $\lambda_c$  are given through [23]:

$$\sum_{i=0}^{\lambda_c} i \cdot p_{\lambda_c, i} = \frac{W^2}{2L}, \quad \text{while} \quad \sum_{i=0}^{\lambda_c} p_{\lambda_c, i} = 1 \quad (3)$$

where the factor  $1/2$  is due to the fact that data-bit “0” is not encoded. For  $\lambda_c = 1$ , the percentage of the total power of another’s user bit that interferes with a bit of the new call is  $1/W$ , since 1 out of  $W$  “1” of the codewords may interfere. In this case  $P_{\text{interf}} = (1/W) p_{\lambda_c, 1} = W/2L$ . In the general case where the maximum value of the cross-correlation is  $\lambda_c \geq 1$  the probability of interference is given by:

$$P_{\text{interf}} = \sum_{i=0}^{\lambda_c} \frac{i}{W} p_{\lambda_c, i} = \frac{W}{2L} \quad (4)$$

The same condition is used at the receiver, when a passive call jumps to an active state. Based on (2), we define the LBP  $lb_k(n_k^1)$  that a service-class  $k$  call is blocked due to the presence of the additive noise, when the number of active calls is  $n_k^1$ :

$$lb_k(n_k^1) = P \left( \frac{I_N}{I_{\max}} > 1 - \sum_{k=1}^K \left( n_k^1 \frac{I_k}{I_{\max}} \cdot P_{\text{interf}} \right) - \frac{I_k}{I_{\max}} \right) \quad (5)$$

or

$$1 - lb_k(n_k^1) = P \left( \frac{I_N}{I_{\max}} \leq 1 - \sum_{k=1}^K \left( n_k^1 \frac{I_k}{I_{\max}} \cdot P_{\text{interf}} \right) - \frac{I_k}{I_{\max}} \right) \quad (6)$$

Since the total additive noise  $I_N$  follows a Gaussian distribution  $(\mu_N, \sigma_N)$ , the variable  $I_N/I_{\max}$ , which is used for the LBP calculation also follows a Gaussian distribution  $(\mu_N/I_{\max}, \sigma_N/I_{\max})$ . Therefore the right-hand side of (6), which is the Cumulative Distribution Function (CDF) of  $I_N/I_{\max}$ , is denoted by  $F_n(x) = P(I_N/I_{\max} \leq x)$  and is given by:

$$F_n(x) = \frac{1}{2} \left( 1 + \text{erf} \left( \frac{x - (\mu_N/I_{\max})}{(\sigma_N/I_{\max})\sqrt{2}} \right) \right) \quad (7)$$

where  $\text{erf}(\bullet)$  is the well-known error function. Using (6) and (7) we can calculate the LBP,  $lb_k(n_k^1)$  by means of the substitution  $x = 1 - \sum_{k=1}^K (n_k^1 \frac{I_k}{I_{\max}} \cdot P_{\text{interf}}) - \frac{I_k}{I_{\max}}$ :

$$lb_k(x) = \begin{cases} 1 - F_n(x), & x \geq 0 \\ 1, & x < 0 \end{cases} \quad (8)$$

### B. The Distribution of the Number of Active and Passive Calls

The following analysis is inspired by the multi-rate ON-OFF model for the call-level performance of a single link, presented in [24], [25], which considers discrete state space. We consider that the PON capacity is  $C_1$ . This is a discrete parameter, since it represents the total number of codewords that can be assigned to the end-users. When a call is at the passive state, it is assumed that it produces a fictitious interference of a fictitious system, with a discrete capacity  $C_2$ . This *passive system* is used to prevent new calls to enter the system when a large number of calls are at the passive state. In order to employ the analysis presented in [24], we use the following notations:

- the total number of codewords assigned to all in-service active calls is denoted by  $j_1$ .
- the total (fictitious) number of codewords assigned to all in-service passive calls is denoted by  $j_2$ .

Based on the analysis presented in the previous section, a new call will be accepted for service if the total number of codewords assigned to all in-service active calls together with the requirements in codewords of the new call, will not exceed  $C_1$ , which is the PON capacity. Moreover, in order to avert the acceptance of new calls when a large number of calls are in the passive state, the requirements in codewords of the new call together with the total number of codewords assigned to all in-service active calls and the number of codewords assigned to all in-service passive calls should not exceed the fictitious PON capacity (which is expressed by the discrete value  $C_2$ ). Based on this analysis, a new service-class  $k$  call will be accepted for service in the system, if it satisfies both the following constraints:

$$j_1 + b_k \leq C_1 \quad \text{and} \quad j_1 + j_2 + b_k \leq C_2 \quad (9)$$

If we denote by  $\Omega$  the set of the permissible states, then the distribution  $\vec{j} = (j_1, j_2)$ , denoted as  $q(\vec{j})$  can be calculated by the proposed two-dimensional approximate recursive formula:

$$\sum_{i=1}^2 \sum_{k=1}^K b_{i,k,s} p_{i,k}(\vec{j}) q(\vec{j} - B_{i,k}) = j_s q(\vec{j}) \quad (10)$$

where

$$\vec{j} \in \Omega \Leftrightarrow \left\{ \left( j_1 \leq C_1 \cap \left( \sum_{s=1}^2 j_s \leq C_2 \right) \right) \right\} \quad (11)$$

The parameter  $s$  refers to the systems ( $s = 1$  indicates the active system,  $s = 2$  the passive system), while  $i$  refers to the states ( $i = 1$  specifies the active state,  $i = 2$  specifies the passive state). Also,

$$b_{i,k,s} = \begin{cases} b_k, & \text{if } s = i \\ 0, & \text{if } s \neq i \end{cases} \quad (12)$$

and  $B_{i,k} = (b_{i,k,1}, b_{i,k,2})$  is the  $i,k$  row of the  $(2K \times 2)$  matrix  $B$ , with elements  $b_{i,k,s}$ . Also,  $p_{i,k}(\vec{j})$  is the utilization of the  $i$ -th system by service-class  $k$ :

$$p_{i,k}(\vec{j}) = \begin{cases} \frac{\lambda_k [1 - lb_k(j_1 - b_k)]}{(1 - v_k) \mu_{1k}} & \text{for } i = 1 \\ \frac{\lambda_k v_k}{(1 - v_k) \mu_{2k}} & \text{for } i = 2 \end{cases} \quad (13)$$

Moreover,  $j_s$  is the occupied capacity of the system:

$$j_s = \sum_{i=1}^2 \sum_{k=1}^K n_k^i b_{i,k,s} \quad (14)$$

**Proof:** In order to derive the recursive formula of (10) we introduce the following notation:

$$\begin{aligned} \vec{n} &= (n^1, n^2), \quad n^i = (n_1^i, n_2^i, \dots, n_K^i), \\ n_{k+}^i &= (n_1^i, \dots, n_k^i + 1, \dots, n_K^i), \\ n_{k-}^i &= (n_1^i, \dots, n_k^i - 1, \dots, n_K^i), \\ \vec{n}_{k+}^1 &= (n_{k+}^1, n^2), \quad \vec{n}_{k+}^2 = (n^1, n_{k+}^2), \\ \vec{n}_{k-}^1 &= (n_{k-}^1, n^2), \quad \vec{n}_{k-}^2 = (n^1, n_{k-}^2) \end{aligned} \quad (15)$$

Having determined the steady state of the system  $\vec{n} = (n^1, n^2)$ , we proceed to the depiction of the transitions from and to state  $\vec{n}$ , as it is shown in Fig. 2. The horizontal axis of the state transition diagram of Fig. 2 reflects the arrivals on new calls and the termination of calls. More specifically, when the system is at state (A) it will jump to state (B) with a rate  $\lambda_k$ , when a new service-class  $k$  call arrives at the system. This rate is multiplied by the probability  $1 - lb_k(n_k^1 - 1)$  that this call will not be blocked due to the presence of the additive noise. Similarly, we define the rate from state (C) to state (A). From state (B) the system will jump to state (A)  $\mu_{1,k}(n_k^1 + 1)(1 - v_k)$  times per unit time, since one of the  $n_k^1 + 1$  active calls of service-class  $k$  (in state (B)) will depart from the system with probability  $(1 - v_k)$ . The transition from state (A) to state (C) is defined in a similar way.

The vertical axis of the state transition diagram of Fig. 2 defines the transition from the active state to the passive state and vice versa. In particular, when the system is at state (A) it will jump to state (D)  $\mu_{2,k} n_k^2 [1 - lb_k(n_k^1)]$  times per unit time. In this case a transition from the passive state to the active state occurs; this transition will be blocked only due to

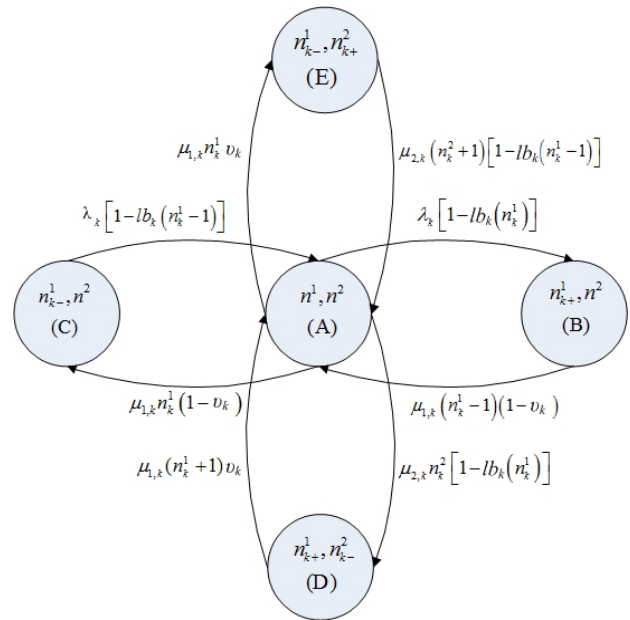


Fig. 2. State transition diagram of the OCDMA system with active and passive users.

the presence of the additive noise, which is expressed by the LBP. The reverse transition (from state (D) to state (A)) occurs when one of  $n_k^1 + 1$  active calls jumps to the passive state with probability  $v_k$ . Similarly, we can define the transitions between states (E) and (A).

Let  $P(\vec{n})$  be the probability of the steady state of the state transition diagram. Assuming that local balance exists between two subsequent states, we derive the local balance equations:

$$\begin{aligned} P(\vec{n}) \mu_{1k} n_k^1 v_k &= P(\vec{n}_{k-+}) \mu_{2k} (n_k^2 + 1) [1 - lb_k(n_k^1 - 1)] \\ P(\vec{n}) \lambda_k [1 - lb_k(n_k^1)] &= P(\vec{n}_{k+}^1) \mu_{1k} (n_k^1 + 1) (1 - v_k) \\ P(\vec{n}) \mu_{2k} n_k^2 [1 - lb_k(n_k^1)] &= P(\vec{n}_{k+}^2) \mu_{1k} (n_k^1 + 1) v_k \\ P(\vec{n}) \mu_{1k} n_k^1 (1 - v_k) &= P(\vec{n}_{k-}^1) \lambda_k [1 - lb_k(n_k^1 - 1)] \end{aligned} \quad (16)$$

We assume that the system of (16) has a Product Form Solution (PFS):

$$P(\vec{n}) = \frac{1}{G} \prod_{i=1}^2 \prod_{k=1}^K \frac{p_{i,k}^{n_k^i}(n_k)}{n_k!} \quad (17)$$

where  $G$  is a normalization constant and  $p_{i,k}(n_k)$  is given by:

$$p_{i,k}(n_k) = \begin{cases} \frac{\lambda_k [1 - lb_k(n_k^1 - 1)]}{(1 - v_k) \mu_{1k}} & \text{for } i = 1 \\ \frac{\lambda_k v_k}{(1 - v_k) \mu_{2k}} & \text{for } i = 2 \end{cases} \quad (18)$$

In order for (17) to satisfy all equations of the system of (16) using (18), we assume that  $1 - lb_k(n_k^1) \approx 1 - lb_k(n_k^1 - 1)$ , i.e. the acceptance of one additional call in active state does not affect the LBP. This is the first assumption that we take into account in order to derive (10). By using (18) and this assumption, the last equation of (16) can be re-written as:

$$n_k^i P(\vec{n}) = p_{i,k}(n_{k-}) P(\vec{n}_{k-}^i) \quad (19)$$

The probability  $q(\vec{j})$  is given by:

$$q(\vec{j}) = P(\vec{j} = \vec{n} \cdot B) = \sum_{\vec{n} \in \Omega_{\vec{j}}} P(\vec{n}) \quad (20)$$

where  $\Omega_{\vec{j}} = \left\{ \vec{n} \in \Omega_{\vec{j}} : \vec{n}B = \vec{j}, n_k^i \geq 0, i=1, 2, k=1, \dots, K \right\}$ . By multiplying both sides of (19) with  $b_{i,k,s}$ , and summing over  $k = 1, \dots, K$  and  $i = 1, 2$ , we have:

$$P(\vec{n}) \sum_{i=1}^2 \sum_{k=1}^K b_{i,k,s} n_k^i = \sum_{i=1}^2 \sum_{k=1}^K b_{i,k,s} p_{i,k}(n_{k-}) P(\vec{n}_{k-}) \quad (21)$$

By using (14) and summing both sides of (21) over the set of all states of  $\Omega_{\vec{j}}$ , we have:

$$j_s \sum_{\vec{n} \in \Omega_{\vec{j}}} P(\vec{n}) = \sum_{i=1}^2 \sum_{k=1}^K b_{i,k,s} p_{i,k} \sum_{\vec{n} \in \Omega_{\vec{j}}} p_{i,k}(n_{k-}) P(\vec{n}_{k-}) \quad (22)$$

The second assumption that we consider is that:

$$\sum_{\vec{n} \in \Omega_{\vec{j}}} p_{i,k}(n_{k-}) P(\vec{n}_{k-}) \approx p_{i,k}(n_{k-}) \sum_{\vec{n} \in \Omega_{\vec{j}}} P(\vec{n}_{k-}) \quad (23)$$

Based on the fact that  $(\vec{n}B = \vec{j}) \Rightarrow (n_{k-}^i B = j - B_{i,k})$ , (18) is equal to (13), and (20) can be rewritten as:

$$q(\vec{j} - B_{i,k}) = \sum_{\vec{n} \in \Omega_{\vec{j}}} P(n_{k-}^i) \quad (24)$$

Finally, we derive the recursive formula of (10), by using the assumption of (23) and substituting (20) and (24) to (23). The LBP is a function of the total interference of the in-service active calls  $j_1$ , i.e.  $lb_k(n_k^1) = lb_k(j_1)$ , since

$$\begin{aligned} x &= 1 - \sum_{k=1}^K (n_k^1 \frac{I_k}{I_{\max}} \cdot P_{\text{interf}}) - \frac{I_k}{I_{\max}} \Leftrightarrow \\ x &= 1 - \sum_{k=1}^K (n_k^1 \frac{b_k \cdot I_{\text{unit}}}{I_{\max}} \cdot P_{\text{interf}}) - \frac{b_k \cdot I_{\text{unit}}}{I_{\max}} \Leftrightarrow \\ x &= 1 - (j_1 \cdot \frac{I_{\text{unit}}}{I_{\max}} \cdot P_{\text{interf}}) - \frac{b_k \cdot I_{\text{unit}}}{I_{\max}} \end{aligned} \quad (25)$$

### C. Performance Metrics

The CBP is calculated by combining LBP and HBP as follows:

$$Pb_k = \sum_{\vec{j} \in \Omega - \Omega_h} lb_k(j_1) q(\vec{j}) + \sum_{\vec{j} \in \Omega_h} G^{-1} q(\vec{j}) \quad (26)$$

where  $\Omega_h = \left\{ \vec{j} \mid [(b_{i,k,1} + j_1) > C_1] \cup [(b_{i,k,2} + j_1 + j_2) > C_2] \right\}$ . The first summation of the right part of (26) refers to the probability that a new call could be blocked at any system state due to the presence of the additive noise. The second summation signifies the HBP, which is derived by summing the probabilities of all the blocking states that are defined by (9). Note that the bounds of the first summation in (26) are

accidentally different than those of the corresponding equation in [17] due to a misprint in (10) of [17].

The calculation of the BBP is based on the fact that burst blocking occurs when a passive call cannot return to the active state. This situation occurs when at least one of the two reasons are valid: the first reason refers to the case where the number of codewords assigned to the call (so that this call could be transferred from passive to active state) together with the number of codewords assigned to all in-service active calls exceeds the capacity of the PON. The effect of this reason can be determined by the number  $n_k^2$  of service-class  $k$  calls in passive state, when the system is at any burst blocking state:

$$\vec{j} \in \Omega^* \Leftrightarrow \left\{ \left( C_1 - b_k + 1 \leq j_1 \leq C_1 \cap \left( \sum_{s=1}^2 j_s \leq C_2 \right) \right) \right\} \quad (27)$$

By multiplying  $n_k^2$  by the corresponding probability  $q(\vec{j})$  and the service rate in the passive state  $\mu_k^2$  we calculate the rate that service-class  $k$  calls depart from a burst blocking state, if it was possible. Then, we sum the rates that a service-class  $k$  call would depart from any burst blocking state:

$$\sum_{\vec{j} \in \Omega^*} n_k^2 q(\vec{j}) \mu_{2k} \quad (28)$$

The second reason refers to the case where a passive call cannot return the active state due to the presence of the additive noise. Following the same procedure resulted in (28), we calculate the sum of the rates that a service-class  $k$  call would depart from any state, except from the burst blocking states. Due to local blocking, however, each rate is multiplied by the corresponding value of  $lb_k(\vec{j})$ :

$$\sum_{\vec{j} \in \{\Omega - \Omega^*\}} n_k^2 lb_k(\vec{j}) q(\vec{j}) \mu_{2k} \quad (29)$$

By normalizing the sum of (28) and (29) (i.e. by taking into account the state-space  $\Omega$ ), we obtain the BBP of service-class  $k$ ,  $B_{b_k}$ :

$$B_{b_k} = \frac{\sum_{\vec{j} \in \Omega^*} n_k^2 q(\vec{j}) \mu_{2k} + \sum_{\vec{j} \in \{\Omega - \Omega^*\}} n_k^2 lb_k(\vec{j}) q(\vec{j}) \mu_{2k}}{\sum_{\vec{j} \in \Omega} n_k^2 q(\vec{j}) \mu_{2k}} \quad (30)$$

The utilization  $\bar{R}_s$  of the shared link  $s$  ( $s=1$  corresponds to the active link and  $s=2$  corresponds to the passive link) is given by:

$$\bar{R}_s = \sum_{i=1}^{C_s} i R_s(i) \quad (31)$$

where  $R_s(i)$  is the marginal link occupancy distribution of the link  $s$  and is given by:

$$R_s(i) = \sum_{\{\vec{j} \mid j_s = i\}} q(\vec{j}) \quad (32)$$

#### IV. SYSTEM MODEL OF A MULTI-RATE OCDMA PON WITH QoS GUARANTEES

In OCDMA networks, QoS differentiation can be realised by the utilization of codewords with different weights. To this end, we assume that the PON supports  $K = T \cdot F$  service-classes:  $F$  service-classes are differentiated by the data rate, while each one of these  $F$  service-classes supports  $T$  different QoS levels that express different values of the BER at the receiver. We also consider that the PON assigns  $(L, W_t, \lambda_a, 1)$  codewords to service-class  $t$ ,  $t = 1, \dots, T$ . Calls of these  $T$  service-classes require the same number  $b_{f,t}$  ( $f = 1, \dots, F$ ) of codewords, while they are differentiated by the weight  $W_t$ . The received power per bit "1" of service-class  $f, t$  is denoted as  $I_{\text{unit}}^{f,t}$ , while the received power that corresponds to a call of service-class  $f, t$  is at most  $I_{f,t}^{\text{act}} = b_{f,t} \cdot I_{\text{unit}}^{f,t}$ . The traffic parameters of service-class  $f, t$  are denoted as  $(\lambda_{f,t}, \mu_{1,f,t}^{-1}, \mu_{2,f,t}^{-1}, v_{f,t})$ . To simplify the presentation of these parameters we use one notation for the service-classes; we denote that the parameters of service-class  $k$  ( $k = 1, \dots, T \cdot F$ ) are  $I_{\text{unit}}^k = I_{\text{unit}}^{f,t}$ ,  $I_{\text{act}}^k = I_{f,t}^{\text{act}}$ ,  $b_k = b_{f,t}$ ,  $\lambda_k = \lambda_{f,t}$ ,  $\mu_{ik}^{-1} = \mu_{i,f,t}^{-1}$  and  $v_k = v_{f,t}$ .

In order to determine the LBP of service-class  $k$ , we use the following relation, which is based on (6):

$$lb_k(n_k^1) = P \left( \frac{I_N}{I_{\text{max}}} > 1 - \sum_{x=1}^{T \cdot F} \left( n_k^1 \frac{b_x \cdot I_{\text{unit}}^x}{I_{\text{max}}} P_{\text{interf}}^{x,k} \right) - \frac{I_{\text{act}}^k}{I_{\text{max}}} \right) \Leftrightarrow$$

$$1 - lb_k(n_k^1) = P \left( \frac{I_N}{I_{\text{max}}} \leq 1 - \sum_{x=1}^{T \cdot F} \left( n_k^1 \frac{b_x \cdot I_{\text{unit}}^x}{I_{\text{max}}} P_{\text{interf}}^{x,k} \right) - \frac{I_{\text{act}}^k}{I_{\text{max}}} \right) \quad (33)$$

where the probability of interference  $P_{\text{interf}}^{x,k}$  between two codewords with weights  $W_x$  and  $W_k$  is a function of the hit probability [26]:

$$p_{x,k} = \frac{W_x W_k}{2L} \quad (34)$$

The probability of interference of a codeword of a service-class  $k$  assigned to a new arriving call and a codeword of service-class  $x$  can be calculated by following the same procedure that was used in order to derive (3):

$$P_{\text{interf}}^{k,x} = \frac{1}{W_x} \frac{W_x \cdot W_k}{2L} = \frac{W_k}{2L} \quad (35)$$

The LBP  $lb_k(j)$  can be calculated by using (8), where the variable  $x$  can be calculated through (33) as follows:

$$x = 1 - \sum_{k=1}^{T \cdot F} \left( n_k^1 \frac{b_k \cdot I_{\text{unit}}^k}{I_{\text{max}}} \cdot P_{\text{interf}}^k \right) - \frac{I_k}{I_{\text{max}}} \Leftrightarrow$$

$$x = 1 - \sum_{k=1}^{T \cdot F} \left( n_k^1 \frac{b_k \cdot I_{\text{unit}}^k}{I_{\text{max}}} \cdot P_{\text{interf}}^k \right) - \frac{b_k \cdot I_{\text{unit}}^k}{I_{\text{max}}} \Leftrightarrow \quad (36)$$

$$x = 1 - \left( \frac{j-1}{I_{\text{max}}} \cdot \sum_{k=1}^{T \cdot F} (P_{\text{interf}}^k \cdot I_{\text{unit}}^k) - \frac{b_k \cdot I_{\text{unit}}^k}{I_{\text{max}}} \right)$$

For the case of the multi-rate OCDMA PON with QoS differentiation the distribution of active and passive calls is given by (10), where the upper bound of the summations that refers to the total number of service-classes has to be changed (from  $K$ ) to  $T \cdot F$ . The same change has to be applied in (26), (30) and (31) in order to calculate the CBP, the BBP and the link utilization, respectively.

#### V. EVALUATION

We evaluate the proposed analytical models through simulation. To this end we simulate the OCDMA PON of Fig.1 by using the Simscript II.5 simulation tool [27]. The simulation results are mean values from 6 runs with confidence interval of 95%. The resulting reliability ranges of the simulation measurements are small and, therefore, we present them only in tables; in figures we provide only mean values. We consider two application examples. In the first example, which is simpler for clarification, we assume that the OCDMA PON supports  $K=2$  service-classes that are only differentiated by the data rate, without QoS differentiation. The PON utilizes the (211,4,1,2) codewords, which result in a maximum number of 105 codewords. Based on the analysis presented in [28] and considering a typical value of BER= $10^{-6}$ , the total number of codewords is reduced to  $C_1$  for  $I_{\text{unit}} = 0.4\mu\text{W}$ . The traffic description parameters of the two service classes are  $(b_1, b_2) = (7, 2)$ ,  $(\mu_{11}^{-1}, \mu_{12}^{-1}) = (0.8, 1.0)$ ,  $(\mu_{21}^{-1}, \mu_{22}^{-1}) = (1.1, 1.4)$ ,  $(v_1, v_2) = (0.9, 0.95)$ . We assume that the maximum received power is equal to  $4 \mu\text{W}$ , while the total number of

TABLE I  
ANALYTICAL VS SIMULATION CBP RESULTS FOR THE 1ST APPLICATION EXAMPLE.

Arrival Rate (calls/sec)	CBP 1 <sup>st</sup> service-class		CBP 2 <sup>nd</sup> service-class	
	Analysis (%)	Simulation (%)	Analysis (%)	Simulation (%)
0.10	0.187	0.183±6.80E-03	0.023	0.023±3.66E-03
0.11	0.309	0.316±1.44E-02	0.041	0.043±3.40E-03
0.12	0.487	0.490±1.65E-02	0.070	0.066±5.93E-03
0.13	0.731	0.715±2.12E-02	0.112	0.110±5.76E-03
0.14	1.056	1.061±2.44E-02	0.172	0.175±8.67E-03
0.15	1.473	1.488±2.91E-02	0.252	0.249±5.15E-03
0.16	1.993	1.995±2.55E-02	0.356	0.3625±4.76E-03
0.17	2.624	2.637±3.89E-02	0.488	0.4789±8.11E-03
0.18	3.371	3.355±5.55E-02	0.648	0.6548±1.17E-02
0.19	4.237	4.118±2.79E-01	0.839	0.8239±5.46E-02
0.20	5.220	5.213±6.16E-02	1.061	1.0773±1.94E-02

TABLE II  
ANALYTICAL VS SIMULATION BBP RESULTS FOR THE 1ST APPLICATION EXAMPLE.

Arrival Rate (calls/sec)	BBP 1 <sup>st</sup> service-class		BBP 2 <sup>nd</sup> service-class	
	Analysis (%)	Simulation (%)	Analysis (%)	Simulation (%)
0.1	6.65E-03	6.5E-03 ± 5.53E-04	8.25E-04	8.69E-04±1.7E-04
0.11	9.91E-03	1.1E-02 ± 1.22E-03	1.27E-03	1.41E-03±1.8E-04
0.12	1.40E-02	1.4E-02 ± 1.27E-03	1.85E-03	1.81E-03±2.4E-04
0.13	1.88E-02	1.9E-02 ± 1.21E-03	2.56E-03	2.43E-03±2.8E-04
0.14	2.43E-02	2.4E-02 ± 1.09E-03	3.42E-03	3.48E-03±3.5E-04
0.15	3.04E-02	2.9E-02 ± 1.10E-03	4.40E-03	4.36E-03±3.3E-04
0.16	3.69E-02	3.7E-02 ± 1.01E-03	5.52E-03	5.78E-03±5.3E-04
0.17	4.37E-02	4.4E-02 ± 1.86E-03	6.74E-03	6.62E-03±3.4E-04
0.18	5.05E-02	5.1E-02 ± 2.55E-03	8.06E-03	8.24E-03±6.9E-04
0.19	5.73E-02	5.7E-02 ± 1.33E-03	9.47E-03	9.60E-03±5.6E-04
0.2	6.38E-02	6.3E-02 ± 1.49E-03	1.10E-02	1.11E-02±5.7E-04

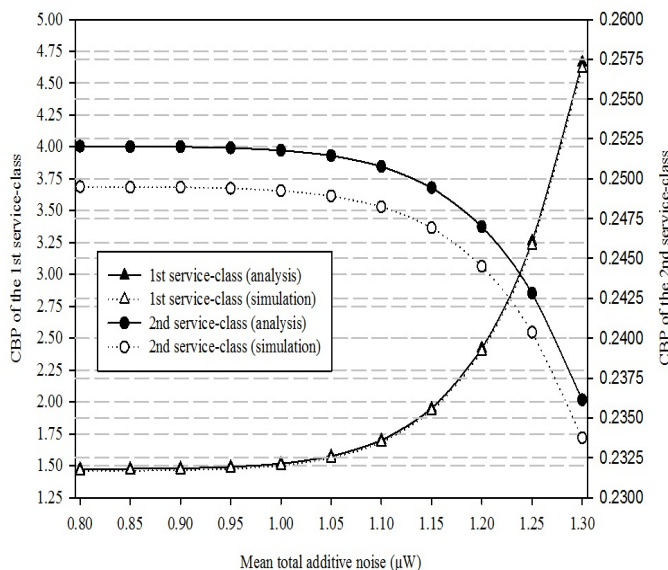


Fig. 3. Analytical and simulation CBP results of the two service-classes versus the mean total additive noise.

fictional codewords is  $C_2 = 45$ . The total additive noise follows a Gauss distribution  $(1, 0.1) \mu W$ .

In Tables I and II, we present analytical and simulation results of the two service-classes for the CBP and BBP, respectively, versus the arrival rate. We assume that the arrival rate is the same for the two service-classes. In Table III we present analytical and simulation results for the utilization of the active and the passive link, versus the arrival rate of the two service-classes. As the results of the three tables reveal, the accuracy of the proposed analysis is absolutely satisfactory.

We also investigate the impact of various network parameters on the CBP and the BBP. To this end, Fig. 3 and 4 present analytical and simulation results of the CBP and the BBP, respectively, for the two service-classes, versus different mean values  $\mu_N$  of the total additive noise, while  $\sigma_N$  is kept constant. In both Fig. 3 and 4 the arrival rate of the two service-classes is  $(0.15, 0.15)$  calls/sec, while the values of all other parameters are the same with those used in Tables I,

TABLE III

ANALYTICAL VS SIMULATION RESULTS FOR THE UTILIZATION OF THE ACTIVE AND THE PASSIVE LINK FOR THE 1ST APPLICATION EXAMPLE.

Arrival Rate (calls/sec)	Active link utilization		Passive link utilization	
	Analysis (%)	Simulation (%)	Analysis (%)	Simulation (%)
0.1	5.594	5.588±8.88E-03	5.827	5.865±1.12E-02
0.11	6.149	6.144±7.35E-03	6.405	6.448±8.56E-03
0.12	6.701	6.699±7.86E-03	6.980	7.029±1.00E-02
0.13	7.249	7.245±1.15E-02	7.550	7.6021±1.46E-02
0.14	7.792	7.783±9.91E-03	8.115	8.1633±1.18E-02
0.15	8.328	8.318±1.14E-02	8.671	8.7234±1.38E-02
0.16	8.855	8.848±9.63E-03	9.219	9.2751±1.18E-02
0.17	9.372	9.363±9.11E-03	9.756	9.8106±1.07E-02
0.18	9.877	9.863±1.07E-02	10.280	10.3317±1.24E-02
0.19	10.370	10.358±1.35E-01	10.789	10.7811±1.55E-01
0.2	10.848	10.837±1.38E-02	11.283	11.3404±1.69E-02

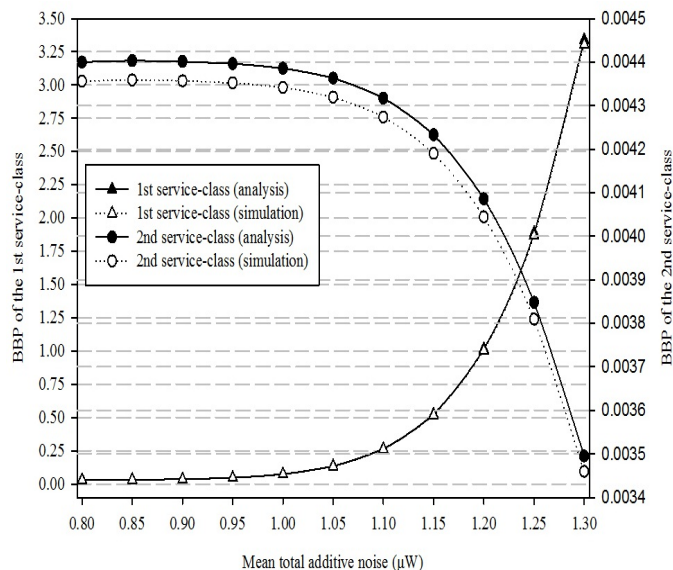


Fig. 4. Analytical and simulation BBP results of the two service-classes versus the mean total additive noise.

II and III. The comparison of analytical and simulation results of Fig. 3 and 4 shows that the accuracy of the proposed model is completely satisfactory for call-level performance. As it is expected from (5) and (6), higher values of the mean total additive noise results in higher values of the LBP and therefore higher values of CBP and BBP. The increase of the mean total additive noise results in the increment of both CBP and BBP of the first service-class, while the values of the CBP and BBP of the second service-class are slightly decreased. This is due to the fact that higher values of the total additive noise increases the LBP; therefore the CBP and the BBP of the first service-class, which has the highest demands in codewords, increases. But in this case more codewords are available for the second service-class, which has lower demands in codewords. Further increase of the mean total additive noise will result in the increase of the CBP and BBP of the second service-class.

Another parameter that we examine is the total interference  $I_{max}$  at the receiver. In Fig. 5 and 6, we present analytical and simulation results for the CBP and BBP, respectively, of the

TABLE IV

ANALYTICAL VS SIMULATION CBP RESULTS OF THE 1ST AND 2ND SERVICE-CLASSES FOR THE 2ND APPLICATION EXAMPLE.

Arrival Rate (calls/sec)	CBP 1 <sup>st</sup> service-class		CBP 2 <sup>nd</sup> service-class	
	Analysis (%)	Simulation (%)	Analysis (%)	Simulation (%)
0.01	0.005	0.005±8.39E-03	0.001	0.001±6.99E-03
0.015	0.056	0.055±2.04E-02	0.009	0.009±1.70E-02
0.02	0.284	0.278±2.62E-02	0.047	0.046±2.18E-02
0.025	0.884	0.867±3.01E-02	0.147	0.144±2.51E-02
0.03	2.037	1.997±3.15E-02	0.348	0.342±2.62E-02
0.035	3.835	3.760±4.80E-02	0.685	0.672±4.00E-02
0.04	6.259	6.138±6.85E-02	1.184	1.161±5.71E-02
0.045	9.208	9.029±3.44E-01	1.856	1.820±2.87E-02
0.05	12.537	12.293±7.60E-02	2.699	2.647±6.34E-02

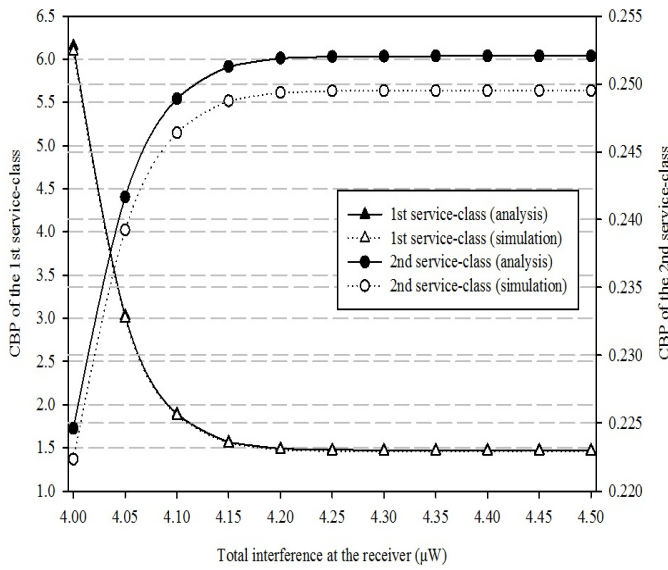


Fig. 5. Analytical and simulation CBP results of the two service-classes versus the total interference.

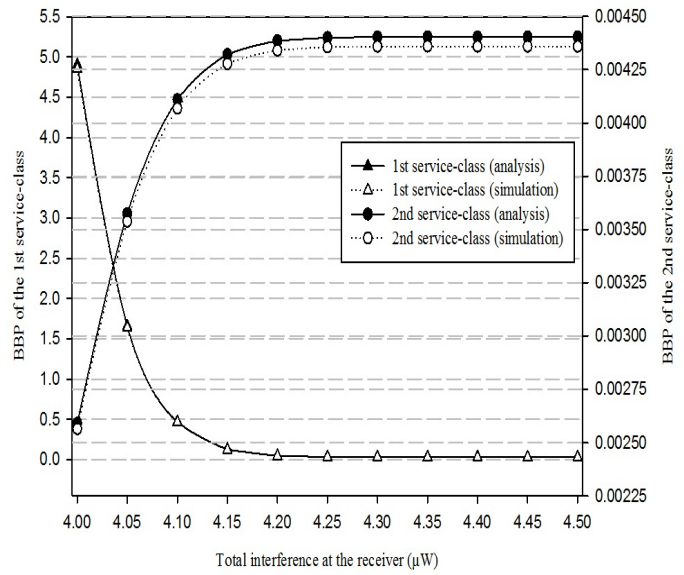


Fig. 6. Analytical and simulation BBP results of the two service-classes versus the total interference.

two service-classes, versus different values of the parameter  $I_{max}$ . In both figures the arrival rate of the two service-classes is (0.15, 0.15) calls/sec, while the values of all other parameters are the same with those used in Tables I, II and III. As the results of Fig. 5 and 6 reveal, the accuracy of the proposed model is absolutely satisfactory, even for small values of the total interference  $I_{max}$ . The decrease of the total interference at the receiver results in higher values of both CBP and BBP of the first service-class, since less interference can be received; therefore less calls of the first service-class can be accommodated at the PON. As in the case of Fig. 3 and 4, this situation results in lower CBP and BBP values of the second service-class, which requires smaller number of codewords. Nevertheless, high values of  $I_{max}$  can be achieved by receivers with higher sensitivity, which are more complicated and therefore more costly.

In order to demonstrate the effect of the fictitious capacity to the CBP and BBP, in Fig. 7 and 8 we present analytical CBP and BBP results, respectively, versus different values of

the total number of fictitious codewords. In both Fig. 7 and 8 the arrival rate of the two service-classes is (0.15, 0.15) calls/sec, while the values of all other parameters are the same as the ones were used previously. The increment of the total number of fictitious codewords results in lower CBP values for both service-classes, since more calls can be accommodated to the passive system. However, this increment results in higher values of the BBP, because the contention for the transition from the passive to the active state. Note that when  $C_1 = C_2$  no burst blocking occurs, but at the expense of higher CBP.

We now proceed to the second application example, which refers to the case of a multi-rate OCDMA PON with QoS differentiation. The PON supports 4 service-classes. Service-classes  $s_1$  and  $s_3$  require the same number of codewords (same data-rate), as well as service-classes  $s_2$  and  $s_4$  require the same number of codewords, but different than that of  $s_1$  and  $s_3$ . Service-classes  $s_1$  and  $s_2$  utilize the (211,4,1,1)-codewords, while service-classes

TABLE V  
ANALYTICAL VS SIMULATION CBP RESULTS OF THE 3RD AND 4TH SERVICE-CLASSES FOR THE 2ND APPLICATION EXAMPLE.

Arrival Rate (calls/sec)	CBP 3 <sup>rd</sup> service-class		CBP 4 <sup>th</sup> service-class	
	Analysis (%)	Simulation (%)	Analysis (%)	Simulation (%)
0.01	0.013	0.012 ± 8.24E-03	0.001	0.001 ± 0.006941
0.015	0.082	0.080 ± 2.00E-02	0.009	0.009 ± 0.01685
0.02	0.342	0.334 ± 2.57E-02	0.047	0.046 ± 0.02165
0.025	0.989	0.967 ± 2.96E-02	0.147	0.144 ± 0.024918
0.03	2.201	2.153 ± 3.09E-02	0.348	0.341 ± 0.026041
0.035	4.063	3.974 ± 4.72E-02	0.685	0.670 ± 0.039726
0.04	6.552	6.408 ± 6.73E-02	1.184	1.158 ± 0.056678
0.045	9.560	9.350 ± 3.38E-01	1.856	1.816 ± 0.28472
0.05	12.537	12.262 ± 7.47E-02	2.699	2.640 ± 0.062908

TABLE VI  
ANALYTICAL VS SIMULATION BBP RESULTS OF THE 1ST AND 2ND SERVICE-CLASSES FOR THE 2ND APPLICATION EXAMPLE.

Arrival Rate (calls/sec)	BBP 1 <sup>st</sup> service-class		BBP 2 <sup>nd</sup> service-class	
	Analysis (%)	Simulation (%)	Analysis (%)	Simulation (%)
0.01	6.36E-05	6.22E-05 ± 1.44E-06	7.79E-06	7.62E-06 ± 1.44E-07
0.015	5.33E-04	5.22E-04 ± 3.50E-06	7.57E-05	7.40E-05 ± 3.50E-07
0.02	2.11E-03	2.06E-03 ± 4.50E-06	3.23E-04	3.16E-04 ± 4.50E-07
0.025	5.52E-03	5.39E-03 ± 5.18E-06	8.78E-04	8.59E-04 ± 5.18E-07
0.03	1.11E-02	1.09E-02 ± 5.41E-06	1.81E-03	1.77E-03 ± 5.41E-07
0.035	1.88E-02	1.84E-02 ± 8.26E-06	3.08E-03	3.01E-03 ± 8.26E-07
0.04	2.81E-02	2.75E-02 ± 1.18E-05	4.60E-03	4.50E-03 ± 1.18E-06
0.045	3.83E-02	3.74E-02 ± 5.92E-05	6.24E-03	6.11E-03 ± 5.92E-06
0.05	4.88E-02	4.77E-02 ± 1.31E-05	7.91E-03	7.74E-03 ± 1.31E-06

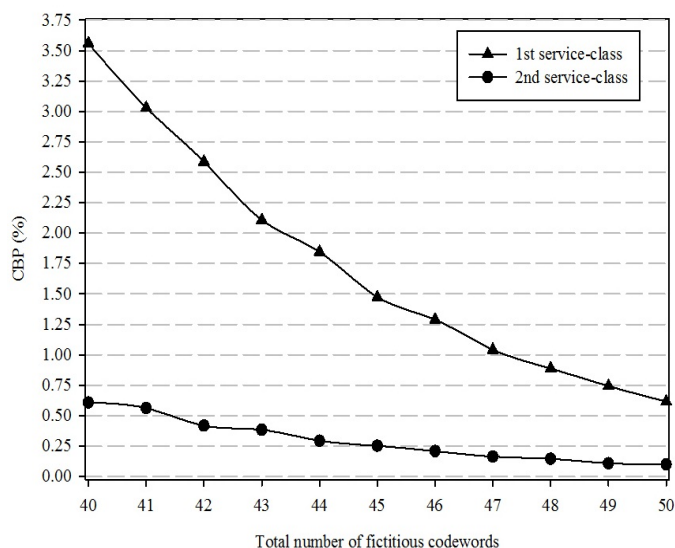


Fig. 7. Analytical CBP results of the two service-classes versus the total number of fictitious codewords.

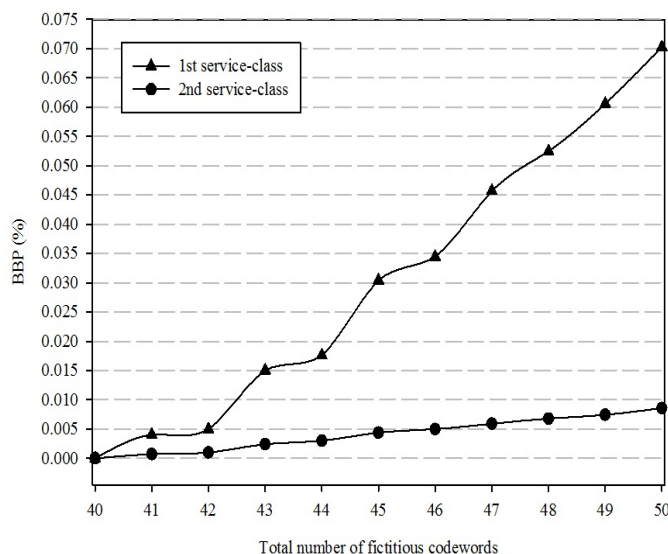


Fig. 8. Analytical BBP results of the two service-classes versus the total number of fictitious codewords.

$s_3$  and  $s_4$  utilize the (211,5,1,1)-codewords. The total number of codewords is assumed to be equal to  $C_1=45$  for  $I_{unit}^1 = I_{unit}^2 = 0.3 \mu W$  and  $I_{unit}^3 = I_{unit}^4 = 0.4 \mu W$ . The traffic description parameters of the 4 service-classes are  $(b_1, b_2, b_3, b_4)=(7,2,7,2), (\mu_{11}^{-1}, \mu_{12}^{-1}, \mu_{13}^{-1}, \mu_{14}^{-1})=(1.0, 1.0, 1.0, 1.1), (\mu_{21}^{-1}, \mu_{22}^{-1}, \mu_{23}^{-1}, \mu_{24}^{-1}) = (1.5, 1.9, 1.5, 1.1), (v_1, v_2, v_3, v_4) = (0.9, 0.9, 0.95, 0.95)$ . The maximum received power at each receiver is assumed to be equal to  $4.0 \mu W$ , while the total number of fictitious codewords is 52. The total additive noise follows a Gauss distribution (1, 0.1)  $\mu W$ .

In Tables IV and V, we present analytical and simulation CBP results of the four service-classes, versus the call arrival rate. Tables VI and VII present analytical and simulation BBP results of the four service-classes, versus the call arrival rate. Also, in Table VIII we present analytical and simulation results for the utilization of the active and the passive link, versus the arrival rate. Comparison between analytical and simulation results shows that the accuracy of the proposed model with QoS differentiation is quite satisfactory. Note that although

the traffic characteristics of service-classes  $s_1$  and  $s_3$  as well as of  $s_2$  and  $s_4$ , justify almost the same CBP and BBP results (the small declinations are due to the effect of the LBP), the obtained results are further differentiated because of the different BER which is expressed by the different codewords.

## VI. CONCLUSION

In conclusion, we present analytical models for the blocking performance of multirate OCDMA PONs with or without QoS guarantees. Our analysis takes into account parameters related to the additive noise, MAI and user activity. We provide and prove an approximate recurrent formula for the efficient calculation of the CBP, which is a function of the LBP, and of the HBP. The accuracy of the proposed analysis is quite satisfactory, as it was verified by simulations. Of course, the efficient applicability of OCDMA technique to PON need further study. As a future work we will incorporate a finite population of traffic sources in the CBP calculation, while we will study the case where the receiver has an interference cancellation capability.

TABLE VII

ANALYTICAL VS SIMULATION BBP RESULTS OF THE 3RD AND 4TH SERVICE-CLASSES FOR THE 2ND APPLICATION EXAMPLE.

Arrival Rate (calls/sec)	BBP 3 <sup>rd</sup> service-class		BBP 4 <sup>th</sup> service-class	
	Analysis (%)	Simulation (%)	Analysis (%)	Simulation (%)
0.01	8.14E-03	7.96E-03 ± 1.98E-04	7.80E-06	7.63E-06 ± 2.92E-04
0.015	2.60E-02	2.55E-02 ± 4.81E-04	7.57E-05	7.40E-05 ± 7.08E-04
0.02	6.00E-02	5.87E-02 ± 6.17E-04	3.23E-04	3.16E-04 ± 9.10E-04
0.025	1.12E-01	1.09E-01 ± 7.11E-04	8.78E-04	8.59E-04 ± 1.05E-03
0.03	1.79E-01	1.75E-01 ± 7.43E-04	1.81E-03	1.77E-03 ± 1.09E-03
0.035	2.56E-01	2.51E-01 ± 1.13E-03	3.08E-03	3.01E-03 ± 1.67E-03
0.04	3.40E-01	3.33E-01 ± 1.62E-03	4.60E-03	4.50E-03 ± 2.38E-03
0.045	4.26E-01	4.17E-01 ± 8.12E-03	6.24E-03	6.11E-03 ± 1.20E-02
0.05	5.10E-01	4.98E-01 ± 1.79E-03	7.90E-03	7.73E-03 ± 2.64E-03

TABLE VIII

ANALYTICAL VS SIMULATION RESULTS FOR THE UTILIZATION OF THE ACTIVE AND THE PASSIVE LINK FOR THE 2ND APPLICATION EXAMPLE.

Arrival Rate (calls/sec)	Active link utilization		Passive link utilization	
	Analysis (%)	Simulation (%)	Analysis (%)	Simulation (%)
0.01	2.7398	2.67968 ± 4.67E+00	4.3648	4.269022 ± 0.013886
0.015	4.1076	4.017466 ± 7.00E+00	6.544	6.400404 ± 0.033708
0.02	5.4658	5.345863 ± 9.32E+00	8.70897	8.517867 ± 0.04331
0.025	6.79756	6.6484 ± 1.16E+01	10.83055	10.59289 ± 0.049847
0.03	8.0781	7.90084 ± 1.38E+01	12.86798	12.58561 ± 0.052094
0.035	9.281585	9.077917 ± 1.58E+01	14.7777	14.45343 ± 0.079469
0.04	10.3875	10.15956 ± 1.77E+01	16.5254	16.16278 ± 0.113382
0.045	11.3842	11.13439 ± 1.94E+01	18.0911	17.69412 ± 0.569564
0.05	12.2689	11.99968 ± 2.09E+01	19.47	19.04277 ± 0.125843

## ACKNOWLEDGMENT

This work was supported by the research program Caratheodory, of the Research Committee of the University of Patras, Greece.

## REFERENCES

- [1] J.S. Vardakas, I.D. Moscholios, M.D. Logothetis, and V.G. Stylianakis, "Blocking performance of Multi-rate OCDMA PONs", in *proc. of the Third International Conference on Emerging Network Intelligence, EMERGING 2011*, November 20-25, 2011, Lisbon, Portugal.
- [2] F. Effenberger, D. Cleary, O. Haran, G. Kramer, R. Li, M. Oron, T. Pfeiffer, "An Introduction to PON Technologies", *IEEE Communications Magazine*, Vol. 45, No. 3, March 2007, pp. S17-S25.
- [3] H. Ueda, K. Okada, B. Ford, G. Mahony, S. Hornung, D. Faulkner, J. Abiven, S. Durel, R. Ballart and J. Erickson, "Deployment status and common technical specifications for a B-PON system", *IEEE Communications Magazine*, Vol.39, No.12, December 2001, pp. 134-141.
- [4] Ethernet in the First Mile Study Group, IEEE std. 802.3ah-2004, 2004 [Online]. Available: <http://www.ieee802.org/3/efm/public/index.html>.
- [5] T. Koonen, "Fiber to the Home/Fiber to the Premises: What, Where, and When?", *Proceedings of the IEEE*, Vol. 94, No. 5, May 2006, pp. 911-934.
- [6] K. Fouli and M. Maier, "OCDMA and Optical Coding- Principles, Applications, and Challenges", *IEEE Communications Magazine*, August 2007, pp. 27-34.
- [7] P. R. Prucnal, *Optical Code Division Multiple Access: Fundamentals and Applications*, New York: Taylor & Francis, 2006.
- [8] M. Azizoglu, J.A. Salehi, and Y. Li, "Optical CDMA via temporal codes", *IEEE Transactions on Communications*, Vol.40, No. 7, July 1992, pp. 1162-1170.
- [9] D. Zaccarin and M. Kavehrad, "An optical CDMA system based on spectral encoding of LED", *IEEE Photonics Technology Letters*, Vol. 5, No. 4, 1993, pp. 479-482.
- [10] M. Morelle, C. Goursaud, A. J.-Vergonjanne, C. A.-Berthelemot, J.-P. Cances, J.-M. Dumas, and P. Guignard, "2-Dimensional optical CDMA system performance with parallel interference cancellation", *Microprocessors and Microsystems*, Vol. 31, No. 4, June 2007, pp. 215-221.
- [11] X. Wang and K. Kitayama, "Analysis of Beat Noise in Coherent and Incoherent Time-Spreading OCDMA", *IEEE/OSA Journal of Lightwave Technology*, Vol. 22, No. 19, October 2004, pp. 2226-2235.
- [12] W.C. Kwong and G.C. Yang, "Multiple-Length extended Carrier-Hopping Prime Codes for Optical CDMA systems supporting Multirate Multimedia services", *IEEE/OSA Journal of Lightwave Technology*, Vol. 23, No. 11, November 2005, pp. 3653-3662.
- [13] E. Intay, H. M. H. Shalaby, P. Fortier, and L. A. Rusch, "Multirate optical fast frequency-hopping CDMA system using power control", *IEEE/OSA Journal of Lightwave Technology*, Vol. 20, No. 2, February 2002, pp. 166-177.
- [14] A.R. Forouzan, N-K. Masoumeh, and N. Rezaee, "Frame Time-Hopping patterns in Multirate Optical CDMA Networks using Conventional and Multicode schemes", *IEEE Transactions on Communications*, Vol. 53, No. 5, May, 2005, pp. 863-875.
- [15] V. Baby, W. C. Kwong, C.-Y. Chang, G.-C. Yang, and P. R. Prucnal, "Performance analysis of variable-weight multilength optical codes for wavelength-time O-CDMA multimedia systems", *IEEE Transactions on Communications*, Vol. 55, No. 6, July 2007, pp. 1325-1333.
- [16] G.-C. Yang, "Variable-weight optical orthogonal codes for CDMA network with multiple performance requirements", *IEEE Transactions on Communications*, Vol. 44, No. 1, January 1996, pp. 47-55.
- [17] J.S. Vardakas, I.L. Anagnostopoulos, I.D. Moscholios, M.D. Logothetis and V.G. Stylianakis, "A Multi-Rate Loss Model for OCDMA PONs", in *Proc. of the 13th ICTON 2011*, Stockholm, Sweden, 26-30 June 2011.
- [18] S. Goldberg and P. R. Prucnal, "On the Teletraffic Capacity of Optical CDMA", *IEEE Transactions on Communications*, Vol. 55, No. 7, July 2007, pp. 1334-1343.
- [19] M. Gharraei, C. Lepers, O. Affes, and P. Gallion, "Teletraffic Capacity Performance of WDM/DS-OCDMA Passive Optical Network", *NEW2AN/ruSMART 2009*, LNCS 5764, Springer-Verlag Berlin Heidelberg, 2009, pp. 132-142.
- [20] J.S. Vardakas, V.G. Vassilakis and M.D. Logothetis, "Call-Level Analysis of Hybrid OCDMA-WDM Passive Optical Networks", in *Proc. of the 10th ICTON 2008*, Athens, Greece, 22-26 July 2008.
- [21] V.G. Vassilakis, G.A. Kallos, I.D. Moscholios, and M.D. Logothetis, "The Wireless Engset Multi-Rate Loss Model for the Call-level Analysis of W-CDMA Networks", in *Proc. of the 8th IEEE PIMRC 2007*, Athens 2007.
- [22] W. Ma, C. Zuo, and J. Lin, "Performance Analysis on Phase-Encoded OCDMA Communication System", *IEEE/OSA Journal of Lightwave Technology*, Vol. 20, No. 5, May 2002, pp. 798-803.
- [23] H.-W. Chen, G.-C. Yang, C.-Y. Chang, T.-C. Lin and W. C. Kwong, "Spectral Efficiency Study of Two Multirate Schemes for Asynchronous Optical CDMA", *IEEE/OSA Journal of Lightwave Technology*, Vol. 27, No.14, July 2009, pp. 2771-2778.
- [24] M. Mehmet Ali, "Call-burst blocking and call admission control in a broadband network with bursty sources", *Performance Evaluation*, Vol. 38, No. 1, September 1999, pp. 1-19.
- [25] I.Moscholios, M. Logothetis and G. Kokkinakis, "Call-burst blocking of ON-OFF traffic sources with retrials under the complete sharing policy", *Performance Evaluation*, Vol. 59, No.4, March 2005, pp. 279-312.
- [26] N. G. Tarhuni, T. O. Korhonen, E. Mutafungwa, and M. S. Elmusrati, "Multiclass Optical Orthogonal Codes for Multiservice Optical CDMA Codes", *IEEE/OSA Journal of Lightwave Technology*, Vol. 24, No. 2, February 2006, pp. 694-704.
- [27] Simscript II.5, <http://www.simscrip.com/>
- [28] C.-S. Weng, and J. Wu, "Optical Orthogonal Codes With Nonideal Cross Correlation", *IEEE/OSA Journal of Lightwave Technology*, Vol. 19, No. 12, December 2001, pp. 1856-1863.